

INTERFACIAL BOND CHARACTERISTICS OF FIBER REINFORCED CEMENTITIOUS MATRIX FOR EXTERNAL STRENGTHENING OF REINFORCED CONCRETE MEMBERS

CHRISTIAN CARLONI^{*}, LESLEY H. SNEED[†] AND TOMMASO D'ANTINO^{††}

^{*} University of Hartford

Department of Architecture, Hartford, CT, USA

e-mail: carloni@hartford.edu, web page: <http://www.hartford.edu>

[†] Missouri University of Science and Technology (Missouri S&T)

Department of Civil, Architectural & Environmental Engineering, Rolla, MO, USA

e-mail: sneedlh@mst.edu, web page: <http://www.mst.edu>

^{††} University of Padova

Department of Civil, Architectural and Environmental Engineering, Padova, Italy

e-mail: tommaso.dantino@dicea.unipd.it, web page: <http://www.unipd.it>

Key words: Fiber Reinforced Cementitious Matrix, Composites, Strengthening

Abstract: This paper presents the results of an experimental study and discusses the applicability of a fracture mechanics based approach to understand the stress transfer mechanism of fiber reinforced cementitious matrix (FRCM) composites externally bonded to a concrete substrate. The FRCM composite was comprised of polyparaphenylene benzobisoxazole (PBO) fibers and polymer-modified cement-based mortar. This research aims to gain insight into the fundamental behavior of the bond between concrete and FRCM composites, which is critical in structural strengthening applications because complete loss of bond (debonding) generally initiates structural member failure. Single lap shear tests were conducted on specimens with composite strips bonded to concrete blocks. Parameters varied were composite bonded length and bonded width. Results were analyzed to understand the effective bond length, which can be used to establish the load-carrying capacity of the interface to design the strengthening system. Results also shed light on the interfacial behavior between fibers and matrix and highlight the role of the matrix in the stress transfer.

1 INTRODUCTION

Fiber-reinforced composite strengthening of RC members is the result of load sharing between the RC member and composite. Load sharing is achieved through load (stress) transfer between the concrete substrate and composite. The performance of composites is usually limited by the matrix-fiber or matrix-substrate interface bond quality, since premature interfacial debonding limits the level of load sharing between composite and concrete substrate.

A critical role in the composite

strengthening technique is played by the type of adhesive (or matrix) used in the composite. The matrix serves as the binder for the fibers and transmits and distributes shear forces between and along the fibers. The matrix also bonds the composite to the concrete substrate, which is necessary for load sharing.

Studies in the literature on the behavior of composites with cement-based matrices show that while this system can be used successfully in structural strengthening applications (shear [1,2], flexure [1,3-9], confinement [10-13]), the performance is different than traditional

FRP composites due to differences in failure mechanisms resulting from complex matrix-fiber bonding characteristics. In FRP composites, debonding typically occurs within the concrete substrate controlled by the low tensile strength of concrete, whereas in cement-based composites, debonding has been observed to occur at the matrix-fiber interface [1,5,6, 14-16]. Debonding has been reported as a progressive process in cement-based composites resulting in larger deformations within the composite material and increased ductility as compared to FRP composites [14]. This aspect can be beneficial in certain structural strengthening or hardening applications that require ductility or energy dissipation. To realize the full benefits of cement-based composites, however, a complete understanding of the mechanism of load transfer and bond behavior is critical to design.

This paper presents the results of an experimental study conducted to understand the stress transfer mechanism of fiber reinforced cementitious matrix (FRCM) composites externally bonded to a concrete substrate. The FRCM composite was comprised of polyparaphenylene benzobisoxazole (PBO) fiber net and polymer-modified cement-based mortar. Results from single lap shear tests with different bonded lengths, bonded widths, and layers of matrix are presented and discussed.

2 EXPERIMENTAL PROGRAM

2.1 Test setup

Single lap shear tests were conducted on concrete block (prism) specimens with an externally-bonded FRCM composite strip of varying bonded length, bonded width, and matrix thickness. The classical push-pull configuration was adopted where the fibers are pulled while the concrete prism is restrained. The dimensions of all concrete prisms were 125 mm width x 125 depth x 375 mm length. The composite material was comprised of bidirectional PBO fiber net and polymer-modified cement-based mortar. The width b^*

and the thickness t^* of one longitudinal fiber bundle were 5mm and 0.046 mm, respectively. The matrix was used only in the bonded region to embed the fibers and bond the composite to the concrete substrate. Fibers were left bare outside the bonded area. Two aluminum plates were attached at the end of the fiber strip to improve gripping during testing (Figure 1).

A steel frame bolted to the testing machine platten was used to restrain the concrete prism. A steel plate was inserted between the steel frame and the top of the prism to distribute the pressure provided by the frame restraint. The distance between two points on each vertical leg of the steel frame was measured before and after tightening the bolts connecting the frame to the platten to evaluate the precompression induced in the concrete prism.

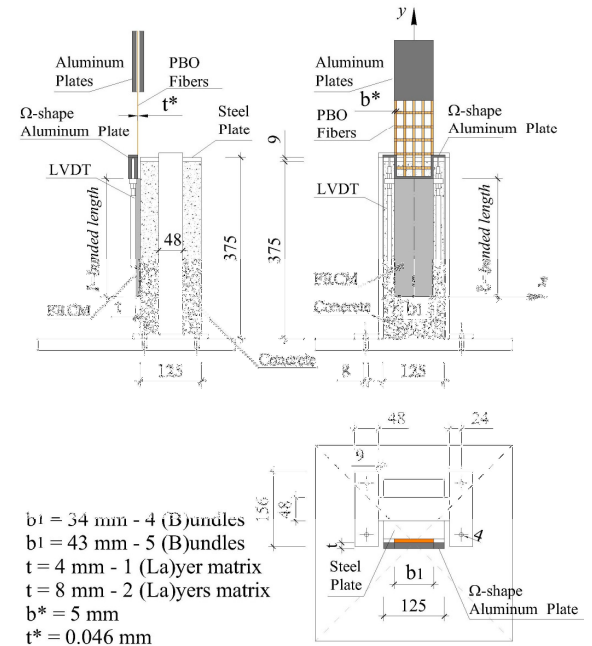


Figure 1: Test setup (dimensions in mm)

Tests were conducted under displacement control using a close-loop servo-hydraulic universal testing machine with a 556 kN force and +/- 150 mm stroke capacity. During testing the global slip, which is defined as the relative displacement between points on the composite strip at the beginning of the bonded area and the concrete prism, was increased at a constant rate of 0.00084 mm/s up to failure. Global slip was measured using two LVDTs

that were attached on the concrete surface close to the edge of the bonded region. The LVDTs reacted off of a thin aluminum Ω -shape plate, which was attached to the PBO transversal fiber bundle surface adjacent to the beginning of the bonded region as shown in Figures 1 and 2.

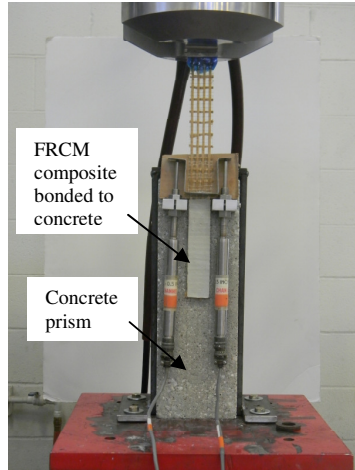


Figure 2: Photo of specimen DS_150_34_1

2.2 Material properties and specimen preparation

The concrete prisms were constructed with normal weight concrete with Portland cement (Type 1) without admixtures. The maximum size of the aggregate was 9.5 mm. Six 100 mm \times 200 mm concrete cylinders were cast from the same batch to determine the concrete compressive strength and splitting tensile strength in accordance with ASTM C39 [17] and ASTM C496 [18]. Results are provided in Table 1.

Table 1: Average mechanical materials properties (CoV)

	Compressive strength [MPa]	Tensile strength [MPa]
Concrete prisms	42.5 (0.013)	3.4 (0.113)
Concrete mortar	27.9 (0.009)	3.6 (0.072)

From the same batch of matrix used to cast the FRCM composite, ten 50 mm \times 100 mm cylinders were cast to determine the compressive and tensile strengths of the matrix

in accordance with ASTM C39 [17] and ASTM C496 [18]. Results are provided in Table 1. As reported by the manufacturer, the PBO fiber has a tensile strength, ultimate strain and elastic modulus of 5.8 GPa, 0.019 and 270 GPa, respectively.

Twenty one direct shear tests were performed to study the bond characteristics and stress-transfer mechanism of the FRCM composite. The parameters considered in this study were the bonded length and width, and the thickness of the top layer of the composite.

Specimens were named following the notation DS_X_Y(S or L)_Z, where X=bonded length (ℓ) in mm, Y=bonded width (b_1) in mm, S=strain gages were mounted on the specimen, L=absence of the top layer of matrix, and Z=specimen number (Table 2). The number of longitudinal bundles B and the presence of one (1 La) or two layers (2 La) of matrix are indicated in Table 2.

Table 2: Test specimen characteristics

Name	b_1 (B)	ℓ	t (La)	P*
	[mm]	[mm]	[mm]	[kN]
DS_100_34_1	34 (4)	100	8 (2)	1.92
DS_100_34_2	34 (4)	100	8 (2)	0.97
DS_100_34_3	34 (4)	100	8 (2)	1.62
DS_150_34_1	34 (4)	150	8 (2)	2.22
DS_150_34_2	34 (4)	150	8 (2)	1.55
DS_150_34_3	34 (4)	150	8 (2)	2.87
DS_150_34_4	34 (4)	150	8 (2)	2.34
DS_250_34_1	34 (4)	250	8 (2)	2.61
DS_250_34_2	34 (4)	250	8 (2)	2.11
DS_250_34_3	34 (4)	250	8 (2)	2.82
DS_330_34_1	34 (4)	330	8 (2)	2.84
DS_330_34_2	34 (4)	330	8 (2)	3.34
DS_330_34_3	34 (4)	330	8 (2)	-
DS_330_43_1	43 (5)	330	8 (2)	4.23
DS_330_43_2	43 (5)	330	8 (2)	4.17
DS_330_43_S_1	43 (5)	330	8 (2)	4.98
DS_330_43_S_2	43 (5)	330	8 (2)	5.11
DS_330_43_L_1	43 (5)	330	4 (1)	4.59
DS_330_43_L_2	43 (5)	330	4 (1)	4.18
DS_330_43_L_3	43 (5)	330	4 (1)	4.43
DS_330_43_L_S_1	43 (5)	330	4 (1)	3.17

The surface of the concrete prisms was sandblasted before applying the composite. A layer of cementitious matrix was then applied

using molds to control width and thickness. A single layer of PBO fiber net was then applied onto the matrix layer pushing the fibers delicately to assure proper impregnation. A second layer of matrix was then applied over the PBO fibers for 17 of the 21 specimens. Each specimen was allowed to cure for at least one week before testing.

3 TEST RESULTS AND DISCUSSION

3.1 Applied load-global slip response

The typical load responses for different bonded lengths and two bonded widths are depicted in Figure 3. The linear response is followed by a non-linear response up to the peak load. The descending post-peak response is characterized by the slippage of the fibers with respect to the matrix. Tests were terminated when a considerable slippage between fibers and matrix was recorded.

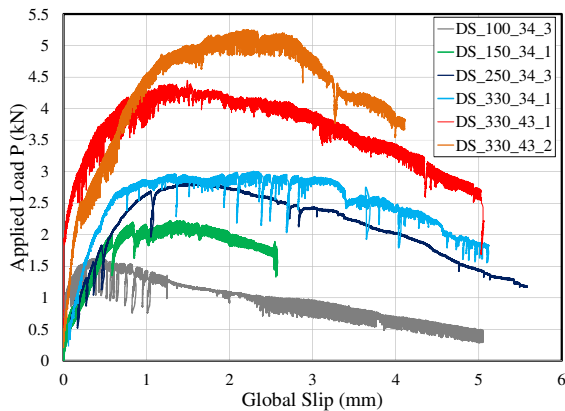


Figure 3: Typical load responses

No damage at the matrix/concrete interface was observed except for specimens DS_100_34_1 and DS_100_34_2. It is possible that a Mode-I condition was prevailing in these two tests due to the short bonded length adopted [19]. Specimens DS_100_34_3, DS_150_34_1, and DS_250_34_3 do not show a constant-load region after the peak load. In the case of FRP-concrete interfaces (joints), a constant-load region entails for self-similar propagation of the interfacial crack that occurs when a bonded length longer than the effective length (L_{STZ})

of the stress transfer zone (STZ) is adopted [20,21]. Specimen DS_330_34_1 shows a constant-load region after the peak load, which can be associated with a bonded length longer than L_{STZ} . Specimen DS_330_34_2 shows a similar response, however the constant-load region corresponds to a smaller range of the global slip. Specimen DS_330_34_3 failed by rupture of the fibers, hence the peak load was not included in Table 2. Specimen DS_330_43_2 shows a constant-load region although corresponding to a limited range of the global slip. A similar trend was observed for specimen DS_330_43_1, although the constant-load region was even smaller than that of specimen DS_330_43_2 in terms of global slip range. It is also possible that specimen DS_330_34_1 had a lower L_{STZ} compared to the other specimens.

Table 2 reports the maximum load P^* , which was calculated as the peak load for those specimens that did not show a constant-load region and as the average of the load in the constant-load region for the others. Figure 4 shows the load P^* normalized with respect of the total width of the fiber bundles Bb^* . If a stress-transfer mechanism similar to the FRP-concrete interface is assumed for FRCM-concrete joints, then from Figures 3 and 4 it is possible to affirm that the effective bonded length L_{STZ} is longer than 250 mm, which confirms the results presented by D'Ambrisi et al [16].

Further data will be available in the near future as this work presents the first sets of data available of a long term experimental study. It will be interesting to study if the effective length is related to the width of the composite, since the fibers are not continuously distributed over the width but instead are concentrated in discrete bundles. Subramaniam et al. [20,21] showed that a central region exists in the case of FRP-concrete joints where the strain, constant across the composite width, should be used to determine fracture parameters included the effective length. The width effect is complicated for FRCM composites by the discrete pattern of the bundles, which could be responsible for a different range of the global

slip where the load is constant. The normalized load P^*/Bb^* for two different widths (corresponding to 4 or 5 bundles) plotted in Figure 4 suggests that a width effect exists, since the load per unit width is higher for specimens with 5 bundles.

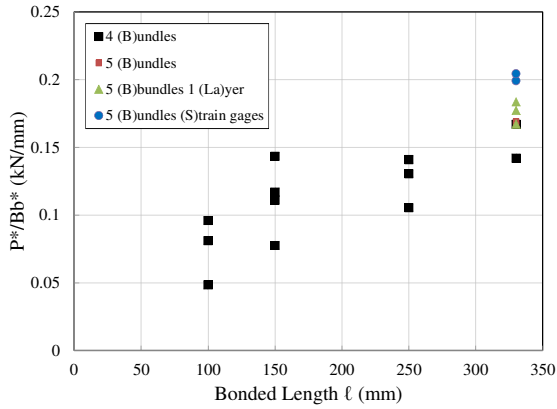


Figure 4: Normalized load P^*/Bb^* versus bonded length

Three specimens (DS_330_43_L_1, DS_330_43_L_2, and DS_330_43_L_3) were cast without the top layer of matrix and tested under the same conditions. A photo of specimen DS_330_43_L_1 is shown in Figure 5. The load responses of those specimens are plotted in Figure 6 in addition to specimens DS_330_34_1, DS_330_43_1, and DS_330_43_2, which included the top layer of matrix, for comparison.

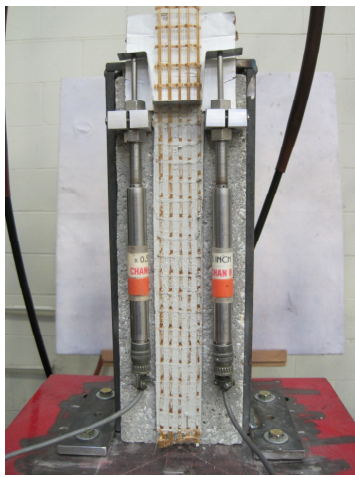


Figure 5: Photo of specimen DS_330_43_L_1

Interestingly the maximum load appears to

be independent of presence of the top matrix layer especially if the average load of specimens DS_330_43_1 and DS_330_43_2 is considered. The presence of a constant-load region is not affected by the absence of the top matrix layer, which could entail that the stress-transfer mechanism is preserved. However, the non-linear pre-peak load is reduced, and a marked drop in the load at the onset of the crack propagation can be observed.

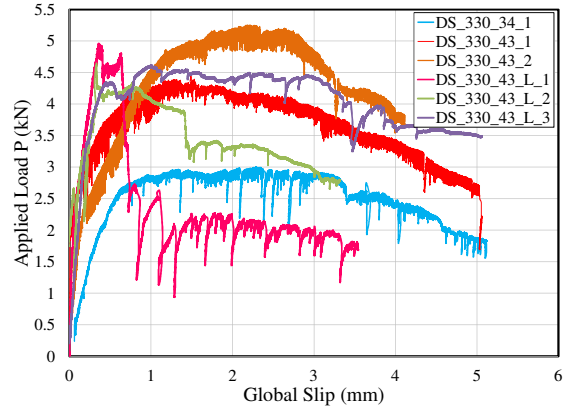


Figure 6: Load responses of specimens without top layer of matrix

The role of the top layer requires further investigation. The debonding mechanism of the composite herein tested appears to occur at the fiber-matrix interface. The top layer of matrix contributes to the constraining action of the fibers, and therefore it is reasonable to assume that the stress-transfer mechanism and the fracture parameters are to some extent affected by the presence of the top layer of matrix. A first attempt to describe the stress-transfer mechanism can be sought in the macro-scale fracture mechanics approach used for FRP-concrete interfaces. D'Ambrisi et al. [15,16] used this approach to analyze their experimental results and determined the associated fracture energy. Additional data are necessary to support the appropriateness of this approach. If a cohesive-material law can be utilized, it will be important to investigate the role of a discrete pattern of bundles and the different thickness of the matrix between FRP and FRCM. In that context, for example, it is possible that the softening portion of the interfacial cohesive law is affected by the

matrix top layer, which in turn would be responsible for the pre-peak load response.

3.2 Strain measurements along the bonded length.

Three specimens (DS_330_43_S_1, DS_330_43_S_2, and DS_330_43_L_S_1) were instrumented with strain gages (gages 4-9) along the bonded length. The strain gages were mounted on the fiber bundles. Slots were created during the application of the top layer of matrix in order to apply the strain gages on the fibers. Three additional strain gages (gages 1-3) were mounted on the central and edge fiber bundles outside the bonded length. A sketch with the names and positions of the strain gages and a photo of specimen DS_330_43_S_2 is shown in Figure 7.

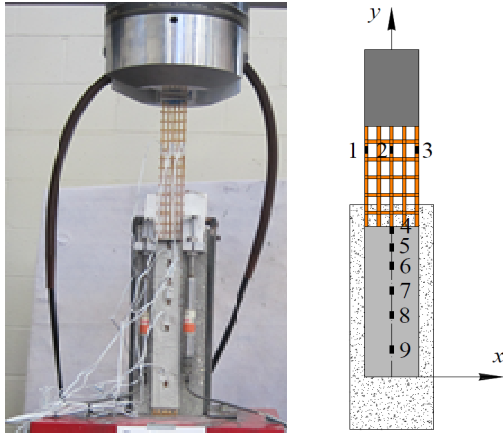


Figure 7: a) Photo of specimen DS_330_43_S_2; b) sketch of the position of the strain gages

The load responses of the specimens with strain gages is reported in Figure 8. The load responses of specimens DS_330_34_1, DS_330_43_1, and DS_330_43_L_3 are also plotted in Figure 8 for comparison. The maximum applied load for specimens DS_330_43_S_1 and DS_330_43_S_2 is consistent with the results previously discussed. However, neither test shows a constant-load region, and the non-linear pre-peak response appears to be more emphasized. It is possible that the slots used to mount the strain gages induced a stress concentration at the gage locations or modified the restraining action of the matrix, which highlights the need

for better understanding of the role of the top layer of matrix as mentioned previously. In future tests, the authors have decided to embed the strain gages in the matrix while still applying them on the fibers. It is worth noticing that specimen DS_330_43_L_S_1 reached a maximum load considerably lower than DS_330_43_L_3 even though the load response presents the same characteristic of the other similar tests. From closer inspection of specimen DS_330_43_L_S_1 after testing, it was observed that the fibers were not well impregnated when compared to the other specimens without the top layer of matrix. This fact could be potentially the reason for a lower maximum load.

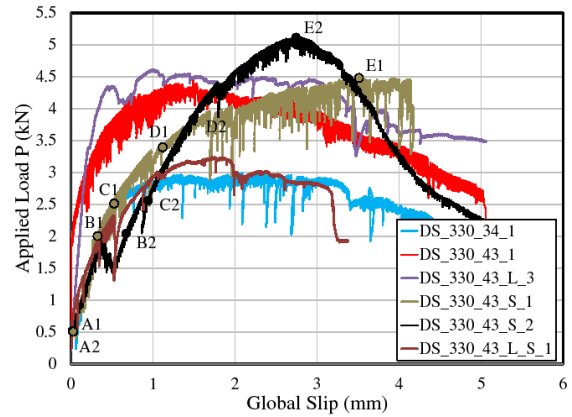


Figure 8: Load responses of specimens with strain gages

The variation of the strain in specimen DS_330_43_S_1 at different locations along the fibers for different values of the load is depicted in Figure 9. Note that location along bonded length y is defined in Figures 1 and 7. Five values of the load, corresponding to five points (A1, B1, C1, D1, and E1) of the load response in Figure 8, were considered. The average of the strain values of gages 1, 2 and 3 outside the bonded area is provided in Figure 9. Strain gage 9 was damaged prior to testing, so it is not shown in the figure.

The strain profiles of Figure 9 resemble the profiles obtained from similar tests for FRP-concrete joints [20,21]. Therefore it seems appropriate, as discussed in the previous section, to study the bond characteristics and stress-transfer mechanism at the fiber-matrix

interface, within the framework of fracture mechanics assuming that a cohesive material law is able to describe the load transfer between fiber and matrix.

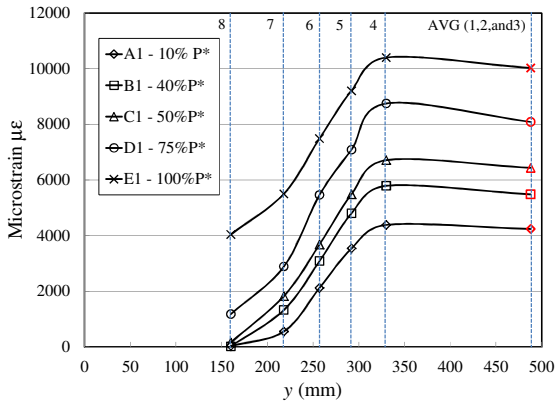


Figure 9: Strain profile along bonded length of specimen DS_330_43_S_1

The strain curve at point E1 indicates that the effective length is longer than the bonded length, which is consistent with the observation that the load response in Figure 8 does not have a constant-load region.

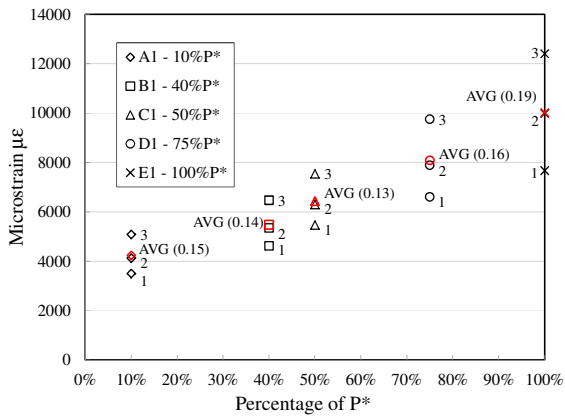


Figure 10: Strain in central and edge bundles of specimen DS_330_43_S_1 outside the bonded region

The strain in the central and edge bundles of specimen DS_330_43_S_1 recorded by gages 1, 2, and 3, outside the bonded region, are reported in Figure 10. The average values used in Figure 9 and the related coefficient of variation are shown in Figure 10. A non-uniform strain distribution is observed among the three bundles. A similar phenomenon is observed in FRP strips attached to concrete,

and it is partially due to the local variation of the interfacial properties. In the case of discrete bundles this phenomenon appears to be more pronounced.

Similarly to Figure 9, the variation of the strain in specimen DS_330_43_S_2 at different locations along the fibers for different values of load is depicted in Figure 11. A strain concentration was recorded by strain gages 4 and 5. Strain fluctuations along the bonded length are to be considered symptomatic of the local variation of the interface properties. The overall trend, however, confirms the discussion of Figure 9.

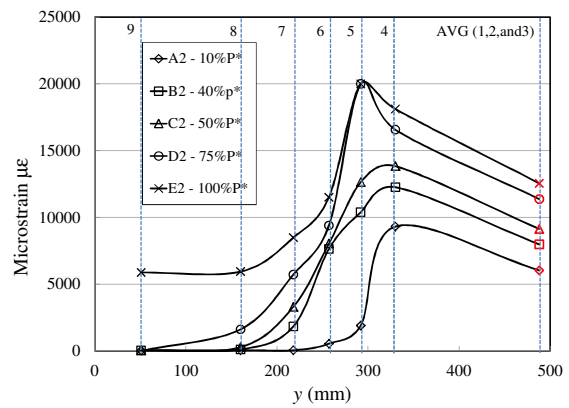


Figure 11: Strain profiles along bonded length of specimen DS_330_43_S_2

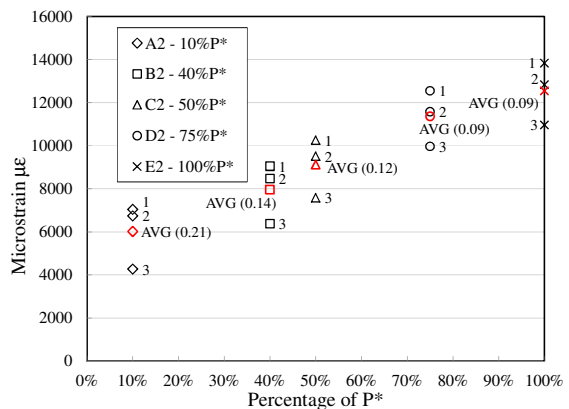


Figure 12: Strain in central and edge bundles of specimen DS_330_43_S_2 outside the bonded region

The strains in the central and edge bundles of specimen DS_330_43_S_2 recorded by gages 1, 2, and 3, outside the bonded region, are reported in Figure 12. The average values used in Figure 11 and the related coefficient of

variation are shown in Figure 12. A non-uniform strain distribution is observed among the three bundles, although the scatter is smaller than that observed in Figure 10 for DS_330_43_S_1. Figures 10 and 12 show a linear relationship between the applied load and the strain in the bundles outside the bonded region. If the average stress of the bundles is computed, the results of Figures 10 and 12 can be used to calculate the elastic modulus of the fibers. Values computed confirm the value provided by the manufacturer.

4 CONCLUSIONS

In this paper the first results of an experimental study are presented to discuss the applicability of a fracture mechanics based model developed to understand the stress transfer mechanism of fiber reinforced cementitious matrix (FRCM) composites externally bonded to a concrete substrate. The FRCM composite was comprised of polyparaphenylene benzobisoxazole (PBO) fibers and polymer-modified cement-based mortar. Direct shear tests using a modified set-up of the classical push-pull configuration were conducted on specimens with composite strips bonded to concrete blocks. Parameters varied were composite bonded length and bonded width, and thickness of the top layer of matrix. The following conclusions can be drawn:

- 1) Debonding occurs at the fiber-matrix interface rather than the matrix-concrete interface,
- 2) The maximum load exhibits a width effect that requires further investigation to understand the role of the discrete fiber bundles embedded in the matrix.
- 3) The strain distribution along the bonded length resembles the strain distribution typical of FRP strips bonded to a concrete substrate. This fact encourages the authors to explore the development of a fracture mechanics model to describe the stress-transfer at the matrix-fiber interface.

ACKNOWLEDGEMENTS

The authors would like to express their appreciation to the National University Transportation Center (NUTC) at Missouri University of Science and Technology for providing financial support for this project. Ruredil S.p.A. of San Donato Milanese, Italy, is gratefully acknowledged for providing the composite materials.

REFERENCES

- [1] Pareek, S., Suzuki, Y., and Kobayashi, A., 2007. Flexural and Shear Strengthening of RC Beams Using Newly Developed CFRP and Polymer-Cement Pastes as Bonding Agents. *Proc. of 8th International Symposium on Fiber Reinforced Polymer Reinforcement for Concrete Structures, FRPRCS-8*, 16-18 July 2007, Patras, Greece.
- [2] Blanksvärd, T., Täljsten, B., and Carolin, A., 2009. Shear Strengthening of Concrete Structures with the Use of Mineral-Based Composites. *J. Compos. Constr.* ASCE **13**(1):25-34.
- [3] Johansson, T. and Täljsten, B., 2005. End Peeling of Mineral Based CFRP Strengthened Concrete Structures – A Parametric Study. In Chen and Teng (eds), *Proc. International Symposium on Bond Behaviour of FRP in Structures (BBFS 2005)*; pp.197-204.
- [4] Orosz, K., Täljsten, B., and Fischer, G., 2007. CFRP Strengthening With Mineral Based Composites Loaded In Shear. *Proc. of 8th International Symposium on Fiber Reinforced Polymer Reinforcement for Concrete Structures, FRPRCS-8*, 16-18 July 2007, Patras, Greece.
- [5] Blanksvärd, T., 2007. Strengthening of Concrete Structures by the Use of Mineral Based Composites. Licentiate thesis, Luleå Univ. of Technology, Luleå, Sweden.

- [6] Täljsten, B., and Blanksvärd, T., 2007. Mineral Based Bonding of Carbon FRP To Strengthen Concrete Structures. *J. Compos. Constr.* ASCE **11**(2):120–128.
- [7] Toutanji, H. and Deng, Y., 2007. Comparison between Organic and Inorganic Matrices for RC Beams Strengthened with Carbon Fiber Sheets. *J. Compos. Constr.* ASCE **11**(5):507–513.
- [8] Ombres, L., 2012. Debonding Analysis of Reinforced Concrete Beams Strengthened with Fibre Reinforced Cementitious Mortar. *Eng. Frac. Mech.* **81**:4–109.
- [9] D'Ambrisi A and Focacci F., 2011. Flexural Strengthening of RC beams with Cement Based Composites. *J. Compos. Constr.* ASCE **15**(2):707–20.
- [10] Ombres, L., 2007. Confinement Effectiveness in Concrete Strengthened with Fiber Reinforced Cement Based Composite Jackets. *Proc. of 8th International Symposium on Fiber Reinforced Polymer Reinforcement for Concrete Structures*, FRPRCS-8, 16-18 July 2007, Patras, Greece.
- [11] Peled, A., 2007. Confinement of Damaged and Nondamaged Structural Concrete with FRP and TRC Sleeves. *J. Compos. Constr.* ASCE **11**(5):514–522.
- [12] Triantafillou, T.C., Papanicolaou, C.G., Zissinopoulos, P., and Laourdekis, T., 2006. Concrete confinement with textile-reinforced mortar jackets. *ACI Struct J.* **103**(1):28–37.
- [13] Bournas, D.A., Triantafillou, T.C., Zygouris, K., and Stavropoulos, F., 2009. Textile-reinforced Mortar Versus FRP Jacketing in Seismic Retrofitting of RC Columns with Continuous or Lap-spliced Deformed Bars. *J. Compos. Constr.* ASCE **13**(5):360–71.
- [14] Wiberg, A., 2003. Strengthening of Concrete Beams Using Cementitious Carbon Fibre Composites. Doctoral thesis, Royal Institute of Technology, Stockholm, Sweden.
- [15] D'Ambrisi, A., Feo, L., and Focacci, F., 2012. Bond-slip Relations for PBO-FRCM Materials Externally Bonded to Concrete. *Compos.: Part B*, <http://dx.doi.org/10.1016/j.compositesb.2012.06.002>.
- [16] D'Ambrisi, A., Feo, L., and Focacci, F., 2012. Experimental Analysis on Bond Between PBO-FRCM Strengthening Materials and Concrete. *Compos.: Part B*, <http://dx.doi.org/10.1016/j.compositesb.2012.03.011>.
- [17] ASTM, 2011. Standard Test Method for Compressive Strength for Cylindrical Concrete Specimens. *C39/C39M-12*, ASTM International, 7 pages.
- [18] ASTM, 2011. Standard Test Method for Splitting Tensile Strength of Cylindrical Concrete Specimens. *C496/C496M* ASTM International, 5 pages.
- [19] Yao, J., Teng, J.G., and Chen, J.F., 2005. Experimental Study on FRP-to-Concrete Bonded Joints. *Composites: Part B* **36**: 99–113.
- [20] Subramaniam, K.V., Carloni, C., and Nobile, L., 2007. Width Effect in the Interface Fracture During Debonding of FRP from Concrete. *Eng. Frac. Mech.* **74**: 578–594.
- [21] Subramaniam, K.V., Carloni, C. and Nobile, L., 2011. An Understanding of the Width Effect in FRP-Concrete Debonding. *Strain* **47**(2):127–137.